RESEARCH PAPER

Monitoring metabolites from *Schizophyllum commune* interacting with *Hypholoma fasciculare* combining LESA–HR mass spectrometry and Raman microscopy

**Riya C. Menezes · Marco Kai · Katrin Krause ·
Christian Matthäus · Aleš Svatoš · Jürgen Popp ·
Erika Kothe**

Abstract Microbial competition for territory and resources is inevitable in habitats with overlap between niches of different species or strains. In fungi, competition is brought about by antagonistic mycelial interactions which alter mycelial morphology, metabolic processes, secondary metabolite release, and extracellular enzyme patterns. Until now, we were not able study in vivo chemical interactions of different colonies growing on the same plate. In this report, we developed a fast and least invasive approach to identify, quantify, and visualize co culture-induced metabolites and their location of release within *Schizophyllum commune*. The pigments indigo, indirubin, and isatin were used as examples to show secondary metabolite production in the interaction zone with *Hypholoma fasciculare*. Using a combinatory approach of Raman spectroscopy imaging, liquid extraction surface analysis (LESA), and high-resolution mass spectrometry, we identified, quantified, and visualized the presence of indigo and indirubin in the interaction zone. This approach allows the investigation of metabolite patterns between wood degrading species in competition to gain insight in community interactions, but could also be applied to other microorganisms. This method advances analysis of living, still developing colonies and are in part not destructive as Raman spectroscopy imaging is implemented.

Keywords Raman spectroscopy · LESA–HRMS · Mass spectrometry pigment production · Indigo · Wood-decaying fungi · Basidiomycetes

R. C. Menezes · K. Krause · E. Kothe
Department of Microbial Communication, Institute of Microbiology, Friedrich Schiller University, Neugasse 25, 07743 Jena, Germany

R. C. Menezes · C. Matthäus · J. Popp
Leibniz Institute of Photonic Technology e.V., Albert Einstein Straße 9, 07745 Jena, Germany

C. Matthäus · J. Popp
Institute of Physical Chemistry and Abbe Center of Photonics, Friedrich Schiller University, Helmholtzweg 4, 07743 Jena, Germany

M. Kai · A. Svatoš (✉)
Research Group Mass Spectrometry, Max Planck Institute for Chemical Ecology, Hans Knöll Straße 8, 07745 Jena, Germany
e-mail: svatos@ice.mpg.de

Introduction

The detection of metabolites usually depends on extraction and purification, solubility tests, absorption spectroscopy, and chemical analyses. Recently, it was shown that mass spectrometric methods (MALDI-MS, nanoDESI-MS) are well suited to study metabolic interactions of microorganisms without extensive sample preparation [1, 2]. Here, we employed two direct analytical techniques, Raman mapping and liquid extraction surface analysis (LESA) combined with high-resolution mass spectrometry (HRMS) to directly examine and localize the metabolites produced upon interaction of *Schizophyllum commune* with other fungi. The Raman spectrum serves as a spectral fingerprint providing comprehensive chemical information for characterization and identification [3, 4]. Confocal micro-Raman spectroscopy allows for direct mapping/imaging combining Raman spectroscopy with light microscopy. LESA is a nanoelectrospray-based, highly reproducible extraction infusion technique for mass spectrometry [5]. Both techniques, confocal micro-Raman spectroscopy

and LESA–HRMS, necessitate only low invasion and are label-free applications requiring minimal sample preparation. Therefore, they are well suited for biological applications [6, 7]. The spatial resolution of a Raman microscope is reported to be in the order of the laser wavelength [8, 9]. While Raman spectroscopy permits the chemical mapping of molecules at a resolution of less than 1 μm, the spatial resolution of LESA–MS can be optimized to ca. 1 mm on tissues such as brain, liver, and kidney, also enabling drug profiling within a single organ [10].

Fungi share important functional roles within ecosystems as nutrient recyclers and decomposers [11] with wood decay fungi being a major component of woodland ecosystems [12]. The white rot basidiomycetes are the dominant group of organisms able to completely decompose all wood lignocellulose components, both in conifer softwood and angiosperm hardwood, including the lignin heteropolymers [13–15]. In their niche, these fungi interact with competitors, which may be other fungi or bacteria. Thereby, mycelial interactions within fungal communities have a significant impact on community structures and nutrient cycling [16].

A sizable body of experimental work has investigated confrontations between wood-decay species, usually paired on agar plates (e.g., [16–19]). Interspecific fungal interactions may be mediated at a distance or by direct contact, and the result of an interaction may include physiological responses like cessation of mycelial extension, barrage formation, increased secretion of enzymes, or pigmentation. In effect, fungi are enabled to defend their territories, thereby restricting access to nutrients for other species [19, 20].

The basis of our study is *S. commune*, a commonly occurring white rot basidiomycete. It has been extensively studied as a model for sexual development in basidiomycetes (see [21] and citations therein), is genetically amenable and the sequence of the genome is available [22]. In an extensive strain collection, pigmented isolates are available that show blue coloration identified as indigo [23, 24]. Other blue pigments reported from fungi include lactarazulene described in *Lactarius deliciosus* [25, 26]; thelephoric acid in members of the genus *Thelephora* and in *Hydnum ferrugineum* [27]; boletol described for *Boletus luridus* and *Boletus satanas* [28] and the blue stain of *Ceratostomella* [29]. Confrontation assays between *S. commune* and *Trichoderma viride* on synthetic media could show changes in metabolite profiles, lipid peroxidation, protein carbonylation, and calcium influx as a result of combat in *S. commune* [30]. However, there was no observation of indigoid derivatives.

Using the combinatory approach of mass spectrometry and Raman spectroscopy, we demonstrate a quick means of low invasiveness to identify, quantify, and image the pigments indigo, indirubin, and isatin in *S. commune* interactions with competing fungi such as *Hypholoma fasciculare* directly from confrontation assays on artificial media. The applied

techniques open up new avenues for further investigations of fungal interactions with co-occurring organisms to obtain more information on their mechanisms, as targets for drug development, or as plant protection agents.

Material and methods

Fungal strains and cultivation All strains are deposited in the Jena Microbial Resource Collection. *S. commune* strains 4–39 (JMRC:FSU:2896), 12–43 (JMRC:FSU:3214), 12–43×4–39, F15 (JMRC:FSU:11842), F28 (JMRC:FSU: 11843), F15× F28; and *H. fasciculare* (JMRC:FSU:11841) were grown on complex yeast medium (CYM: 2 % glucose, 0.2 % trypticase peptone, 0.2 % yeast extract, 0.05 % $MgSO_4 \cdot 7H_2O$, 0.05 % KH_2PO_4, 0.1 % K_2HPO_4, and 1.8 % agar [31]), and potato dextrose agar (PDA: 0.4 % potato extract, 2 % glucose, and 1.5 % agar) at 28 °C for 1 week. For confrontation assays, *S. commune* and *H. fasciculare* were transferred to fresh media in 5 mm^2 pieces placed 5 cm apart on the surface of CYM or potato dextrose agar and incubated at 10 and 28 °C for 1 month.

Microscopy and Raman microspectroscopy Microscopy was carried out with an Axioplan 2 microscope (Carl Zeiss, Jena, Germany). Documentation was achieved with a digital camera (Insight Firewire 4 image sample, Diagnostic Instruments, Sterling Heights) and analyzed by the software Spot (version 4.6, Diagnostic Instruments, Sterling Heights).

Raman spectra were acquired using a WITec (Ulm, Germany) CRM Alpha-300Rplus confocal Raman microscope. Excitation (ca. 10 mW at the sample) was provided by 785 nm diode laser (TOPTICA Photonics AG). The exciting laser radiation is coupled into a Zeiss microscope through a wavelength-specific single-mode optical fiber. The incident laser beam is collimated via an achromatic lens and passes a holographic band pass filter before it is focused onto the sample through the objective of the microscope. A Zeiss 50×/0.9 NA objective was used in the studies reported here. The sample is located on a piezo-electrically driven microscope scanning stage with an x,y-resolution of about 3 nm and a repeatability of ±5 nm, and z-resolution of about 0.3 nm and ±2 nm repeatability. The sample is scanned through the laser focus in a continuous line scan at a constant stage speed of fractions of a micrometer per second. Spectra are collected with a 0.33-μm step size and an illumination time of 3 s, using a 300/mm grating. The spectral resolution is about 6 cm^{-1} and the spectral window ranges from 300 to 3200 cm^{-1}. False color images were reconstructed using a spectral unmixing algorithm based on vertex component analysis (VCA), which decomposes a given dataset into fractions of most dissimilar spectral information [32, 33].

Raman spectra of indigo, isatin, and indirubin (Sigma Aldrich, Taufkirchen, Germany) were used as references. Spectra were processed with the CytoSpec (Berlin, Germany) v. 1.4.00 software developed for hyper spectral imaging and the MATLAB (Mathworks Inc.) software. For intensity plots of the Raman maps, the spectra were baseline corrected and approximated by linear segments with manually chosen points. For sample preparation, $0.5 \times 0.5 \times 0.3$ cm^3 cubes of agar with hyphal mat were cut out from the interaction zones of the culture plates and placed on CaF$_2$ objective slides for Raman microspectroscopic measurements. The samples were trimmed in dimensions (when necessary) to accommodate them within the working distance of the microscope objective.

Metabolite extraction From the co-cultured plates, $4 \times 1 \times 0.3$ cm^3 mycelial strips were cut from the interaction zone and from the periphery of *S. commune* and *H. fasciculare* zones, respectively. Each sample was added into a 1:1 (2 ml each) mixture of methanol:ethyl acetate and macerated. They were then ultrasonicated for 30 min and centrifuged at 10,000 rpm for 3 min. A 500-μl volume of the clear supernatant was retrieved and added to an equal amount of methanol along with 2 μl of 10 mM indole-3-propionic acid (internal standard) in methanol. This mixture was vortexed for 30 s and allowed to stand for 30 min. It was then diluted 1:4 in methanol.

UHPLC–ESI–MS/MS and LESA–MS/MS Liquid extraction surface analysis (LESA) was performed using Triversa Nanomate technology (Advion, Ithaca, NY, USA). For LESA, the confrontation zone on assay plates was directly extracted with 2 μl ethyl acetate in the Nanomate. After 8 s extraction time, 2.2 μl of solvent was aspirated and this extract was further ionized by nanoelectrospray using a voltage of 2 kV at a gas pressure of 0.5 psi. Positive ion mode was used.

Ultra-high-performance liquid chromatography–electrospray ionization–tandem mass spectrometry (UHPLC–ESI–MS/MS) was performed with the diluted extract (see metabolite extraction) using the Ultimate 3000 series RSLC (Dionex, Sunnyvale, CA, USA) system coupled to an LTQ Orbitrap XL mass spectrometer (Thermo Fisher Scientific, Bremen, Germany) equipped with an ESI source. A 15-μl volume of the extract was injected into the UHPLC binary solvent system of water (solvent A) and acetonitrile (solvent B, hypergrade for LC–MS, Merck, Darmstadt, Germany), both containing 0.1 % (*v/v*) formic acid (eluent additive for LC–MS, Sigma Aldrich, Steinheim, Germany). Chromatographic separation was achieved using an Acclaim C18 Column (150×2.1 mm, 2.2 μm; Dionex, Sunnyvale, CA, USA) at a constant flow rate of 300 μl min^{-1} as follows: 0.5–10 % (*v/v*) B (10 min), 10–80 % B (4 min), 80 % B (5 min), 80–0.5 % (*v/v*) B (0.1 min), 0.5 % B (6 min). ESI source parameters were set to 35 V for capillary voltage, 4 kV for spray voltage, and 275 °C for capillary temperature.

The samples were measured in positive ion mode in the range of *m/z* 100–1200 using the LTQ Orbitrap XL analyzer. Full scan mass spectra were generated using 30,000 m/Δm resolving power. Tandem mass spectra of all compounds with the exception of isatin were acquired using collision-induced dissociation in the LTQ trap with relative collision energies of 15, 25, and 35 % at 7500 m/Δm resolving power. Tandem mass spectra of isatin were acquired with the Q Exactive Plus Hybrid Quadrupole-Orbitrap mass spectrometer (Thermo Fisher Scientific, Bremen, Germany) using 70,000 m/Δm resolving power and a higher collision energy of 110 arb. units.

Data analysis was accomplished using XCALIBUR (Thermo Fisher Scientific, Waltham, MA, USA). In addition to mass of precursors, fragmentation patterns as well as retention time (UHPLC) were compared to those of reference compounds. Quantification was performed using calibration curves of reference compounds and the internal standard indole-3-propionic acid. Indigo and indirubin were first dissolved in ethyl acetate and then methanol to make the standard solutions of concentrations 1.54 nM (1.54, 3.85, 7.7, 11.55, and 15.4 pmol) and 15.4 nM (15.4, 38.5, 77.0, 115.5, and 154.0 pmol), and 0.62 pM (0.62, 1.56, 3.12, 6.25, and 9.37 pmol), and 6.25 nM (6.25, 15.62, 31.25, 46.87, and 62.5 pmol), respectively. A 100 nM (100, 250, 300, 400, 500, and 750 pmol) solution of isatin in methanol was prepared. Peak areas from the extracted ion chromatograms corresponding to the parent ions 263.07 (indigo), 263.07 (indirubin), and 148.03 (isatin) were used as a measure of the quantity of the compounds. Principal component analysis (PCA) was executed with MetaboAnalyst 2.0., a web-based tool for metabolomic data processing, statistical analysis, and functional interpretation [34]. PCA was performed on the full-scan data of the samples. The raw spectra were first converted to mzXML format using the MS Convert feature of ProteoWizard 3.0.3750. Data processing was subsequently carried out with R Studio 0.96.316 using the Bioconductor XCMS package which contains algorithms for peak detection, peak deconvolution and peak alignment. This results in a compilation of a list of mz, mzmin, mzmax, rt, rtmin, rtmax, and peak intensities/areas. This file was uploaded into Metaboanalyst as a peak intensity table, the values were normalized and then visualized with PCA.

Results

Interaction of *S. commune* and *H. fasciculare*

To investigate the interaction between *S. commune* and *H. fasciculare*, agar plate-based confrontation assays were performed. While in self-paired cultures both fungi did not exhibit induction of pigmentation, colored substances and

discoloration of the media was observed when *S. commune* interacted with *H. fasciculare* (Fig. 1). The response of *S. commune* to *H. fasciculare* at 10 °C was initiated by cessation of growth and formation of mycelial barrage at 24 and 48 h post contact, respectively. A greenish blue/ sometimes black pigment developed at the bottom of the plate within the domain occupied by *S. commune* at 12 h post contact. The intensity of this pigmentation increased with the duration of contact. After about 15 days of contact, *S. commune* gradually overgrew *H. fasciculare* resulting in partial replacement. The pigmentation was visible in the interaction zones of the fungi on both media used. Microscopic observations showed the presence of blue crystals in the media surrounding the hyphae and within the hyphae of *S. commune* (Fig. 1C–F). *H. fasciculare* did not show signs of blue pigmentation. The pigment produced small crystals of variable shapes in the agar. Time-lapse studies showed that growth of the pigment-filled *S. commune* hyphae ceased once the pigment was produced. New aerial hyphae then were formed, which grew over the region of the excreted pigment, and continued to grow normally.

Analysis of co-cultivation of *S. commune* with *H. fasciculare* for release of indigo using LESA–MS and UHPLC–ESI–MS/MS

A characteristic feature of the interaction zone has been the blue coloration in this area. In order to evaluate LESA–HRMS as a suitable technique for identification of the blue constituents in the competing zone, LESA–HRMS was performed on the confrontation assay plates directly from the surface of the agar (Fig. 2a). Therefore, areas from *S. commune*, *H. fasciculare*, and their interaction zone were sampled.

After data processing and PCA, the acquired mass spectra of every area was distributed into clusters based on similarity. Cluster analysis showed that the metabolites detected from the three zones were completely dissimilar as seen in Fig 2b. Furthermore, the mass spectral data revealed mass signals corresponding to indigo, indirubin, an isobar of indigo, and isatin (Fig 2c). The accurate mass measured for the ions were m/z 263.0807 $[M+H]^+$ with a mass difference of 2.9 ppm to exact mass of protonated indigo and indirubin (calculated for $C_{16}H_{11}N_2O_2$, 263.0815) and m/z 148.0389 $[M+H]^+$ with a mass difference of 2.9 ppm to exact mass of protonated isatin (calculated for $C_8H_6NO_2$, 148.0393). In order to confirm the presence of the respective molecules, the MS/MS spectra of the parent ion signals were acquired and compared with the MS/MS spectrum of pure standards (see Electronic Supplementary Material (ESM) Fig. S1 A, B, C). While it was not possible to acquire fragmentation patterns for isatin (m/z 148.03), the MS/MS spectrum of the parent mass ion m/z 263.08 showed high similarity to the MS/MS spectra of pure indigo and indirubin. Fragment ion peaks were detected at m/z 219.09, 235.09, and 245.07. The same fragments were observed from both reference compounds. The indigo/indirubin mass signal was not visible when extracting and analyzing compounds from zones beneath the mycelium at the periphery of *S. commune* and *H. fasciculare* cultures (Fig. 2c) and neither from the self-paired cultures.

To finally confirm the presence of isatin and indigo and to distinguish the signal from isobaric indirubin, UHPLC–ESI–MS/MS measurements were conducted. Therefore, the compounds present in the agar were extracted from different, defined zones of co- and mono-cultivated culture plates with methanol/ethyl acetate. In the extract obtained from the interaction zone, we could determine two peaks with identical mass

Fig. 1 Pigments visible in and between hyphae in fungal interactions. **a** *S. commune* 12–43×4–39 (*left*) and *H. fasciculare* (*right*) showing pigmentation in zone of contact. **b** Self-paired cultures of *S. commune*, **c** Pigmentation in the interaction zone of *S. commune* 4–39 (*left*) and *H. fasciculare* (*right*), **d** Pigment localized in *S. commune* 12–43×4–39 hyphae in interaction with *H. fasciculare*. **e** Pigment crystals excreted by Δgap mutant strain of *S. commune* F15 into the media, and **f** pigmented hyphae of *S. commune* F15 with pigment secretions in the medium
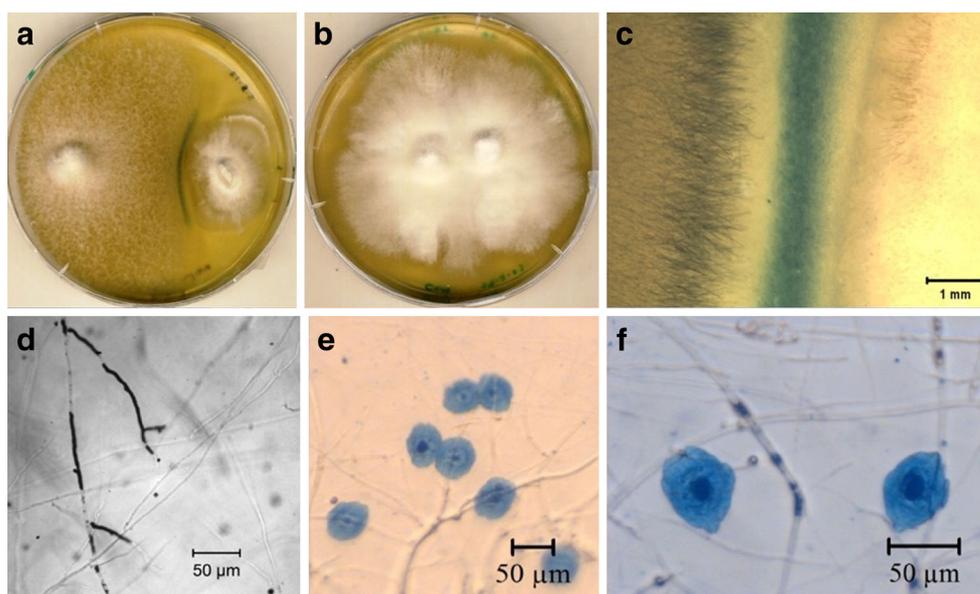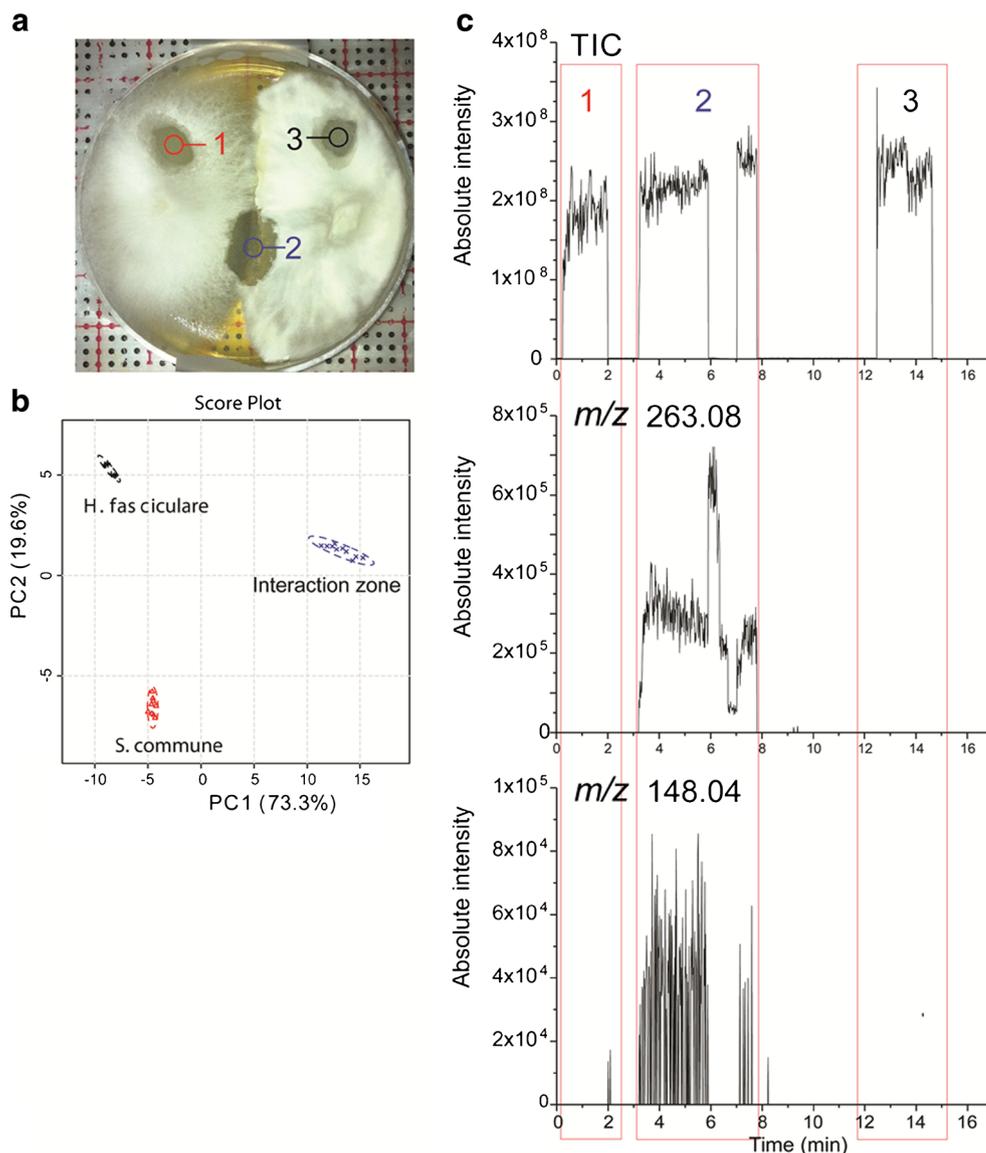
Fig. 2 Co-cultivated strains of *S. commune* and *H. fasciculare* were analyzed for release of indigo using LESA–MS and UHPLC–ESI–MS/MS. **a** Confrontation assay of *S. commune* and *H. fasciculare* after LESA–MS analysis highlighting the investigation zones with numbers: (*1*) zone beneath *S. commune*, (*2*) interaction zone between the fungi, and (*3*) zone beneath *H. fasciculare*. **b** PCA of zone beneath *S. commune* (*red*), zone beneath *H. fasciculare* (*black*), and interaction zone (*blue*). **c** LESA–MS ion intensity acquisition plots of the confrontation assay are depicted. The total ion trace (*upper*) and the selected ion traces of fungal indigo (*m/z* 263.078–263.084 in the middle plot) and isatin (148.03–148.05 in lower plot). The *numbers of the boxes* correspond to zones in (**a**)
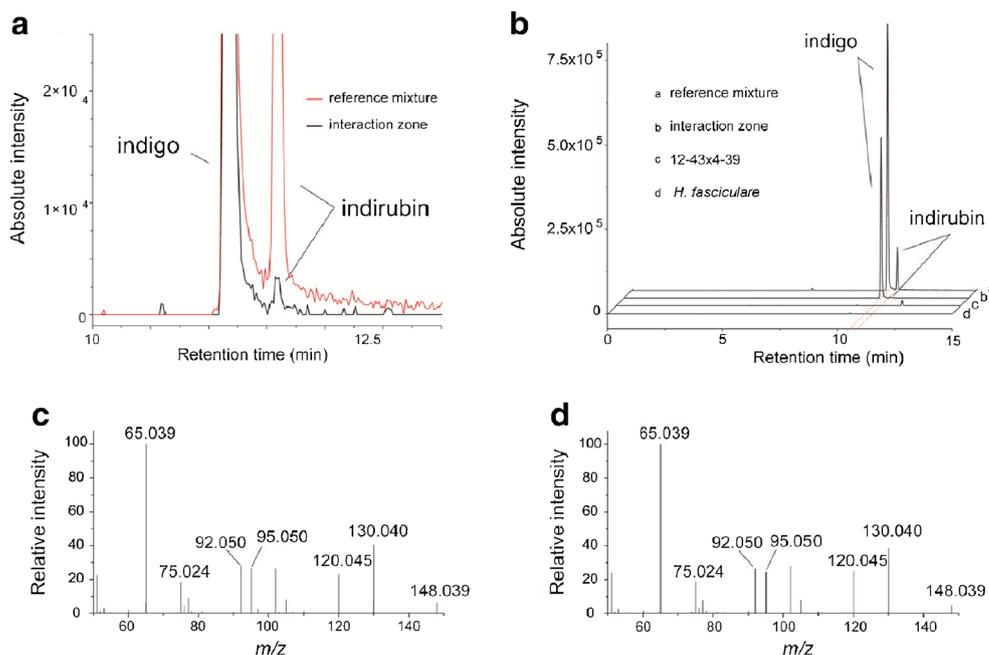
m/z 263.0813 $[M+H]^+$. By comparing the retention times and mass spectra, the more intensive peak has been assigned to protonated indigo while the less intensive peak has been assigned to protonated indirubin (Fig. 3a). Quantification using calibration curves of reference compounds revealed 208±66.76 pmol indigo and 0.87±0.23 pmol indirubin per cm^3 agar to be present in the interaction zone. Analyzing at a detection limit of ca. 300 nmol of isatin, only single scans were detected at *m/z* 148.0391 $[M+H]^+$ with a mass difference of 1.1 ppm to the exact mass of protonated isatin. Whereas it was not possible to observe fragments of isatin in the LTQ Orbitrap MS/MS experiment, product ions of protonated isatin were obtained both in the sample and reference compound at *m/z* 65.04, 75.02, 95.05, and 130.04 with the Q Exactive Plus mass spectrometer (Fig. 3c, d). Finally, neither the *S. commune* strain 12–43×4–39 nor *H. fasciculare* grown alone showed a signal for indigo, indirubin, or isatin. No matrix effects were observed.

Raman spectroscopy For the spectroscopic identification and imaging of the produced pigments, Raman microscopic images were obtained from individual hyphae. Figure 4A shows a microscopic image of a typical *S. commune* hypha grown under normal, non-competing, conditions. The resulting Raman image in 4B was reconstructed by plotting the integrated scattering intensities of the CH stretching vibrations of the hyphal components. The Raman image in 4C was generated by a spectral unmixing algorithm that decomposed the dataset into representative spectra and their individual abundance within the dataset. The associated spectral information (a and b in Fig. 4D) show mainly Raman bands that are characteristic for glycogen or polysaccharides in general and proteins for both plots. Reference spectra for glycogen and a protein (albumin) are given (c and d in Fig. 4D).

Fungal cell walls contain chitin and glucans [35] which also are represented in the Raman spectra. All main Raman

Fig. 3 For confirmation of indigo/indirubin and isatin production, UHPLC–ESI–MS/MS analysis was accomplished. **a** and **b** show the plots of extracted ion chromatograms (EIC) for mass trace of indigo and indirubin respectively (m/z 263.078–263.084). **c** depicts the MS/MS of isatin in the sample that is similar to reference isatin shown in **d**
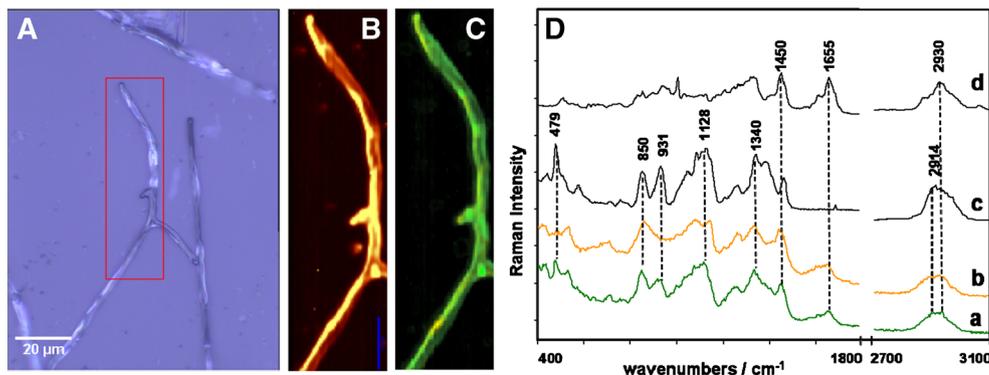

bands can be assigned to spectral features of either polysaccharides, proteins or, in the presence of nuclei, nucleic acids. However, the composition of polysaccharides and proteins varies along the hyphae as indicated by the spectral differences associated with the green and yellow regions.

The Raman bands of the polysaccharides can be assigned to different deformations of the glucose ring fractions. The main protein bands are for instance due to the carbonyl C=O stretching vibrations of the peptide backbone at 1665 cm^{-1}, often referred to as amide I band, or the CH$_2$ scissoring vibrations at 1450 cm^{-1}. The amide III mode at 1331 cm^{-1} is another coupled vibration of the polypeptide backbone, mainly resulting from the coupled C–N stretching and N–H bending motions [36]. The Raman band located at 1654 cm^{-1} results from a superposition of protein, lipid, and polysaccharide vibrations and is therefore a marker of all relevant cell substances, i.e., is typical for the fungal cell matrix [3]. The Raman bands of polysaccharides and proteins have been described in detail [36–38].

Point spectra were taken from *S. commune* hyphae, *H. fasciculare* hyphae and agar medium from the zone of interaction. Raman mapping of *S. commune* hyphae from these zones showed localization of the pigment. On analysis of the hyphae of the fungi with Raman microspectroscopy, the profile of indigo bands was recognized with reference to the pure standard (Fig. 5). The VCA algorithm was again used for spectral analysis of the Raman maps and image generation. Analysis of spectra of the samples taken from the interaction zone revealed that the most intense signal of the ring stretching mode is observed near 1573 cm^{-1} with a pronounced shoulder at 1581 cm^{-1} due to the stretching vibrations of the conjugated system of C=C, C=O, and N–H groups [39]. The vibration of this conjugated system gives rise also to bands near 1363, 1622, and 1700 cm^{-1}. The band attributed to N–H rocking vibration is observed at about 1224 cm^{-1}. Vibrations involving C–H rocking are recognized at 1247, 1459, and 1481 cm^{-1}, while the vibrations of five- and six-membered rings are observed at 756 and 1309 cm^{-1}.

Fig. 4 **A** Light microscopy image of *S. commune* 12–34×4–39 hyphae **B** Raman image of a hypha **C** Pseudo-colored Raman image using a VCA algorithm **D** Raman spectra (**a** and **b**) of the fungal matrix plotted in (**c**) in corresponding colors, (**c**) and (**d**) show reference spectra of glycogen and proteins, respectively
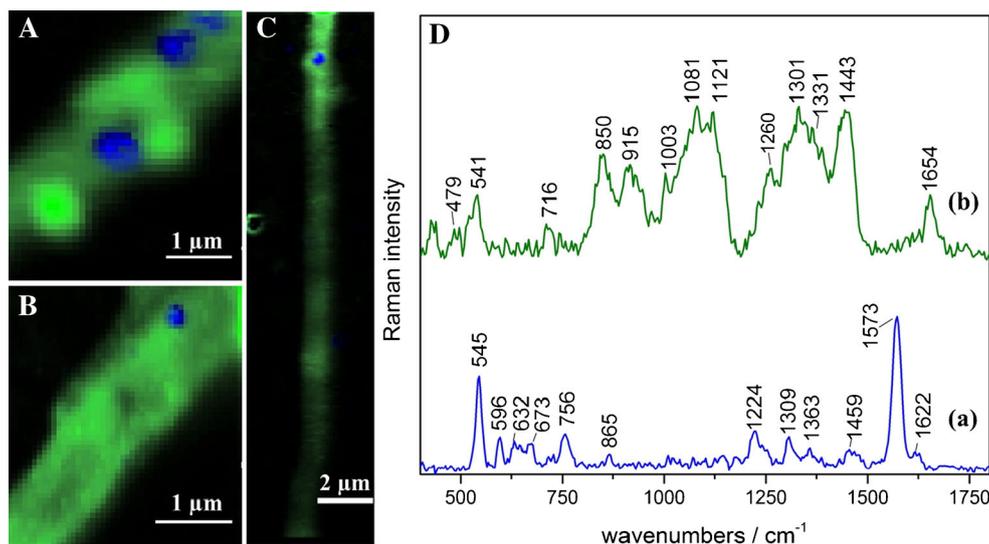
Fig. 5 Pseudo-color Raman maps based on Raman data recorded from three samples showing distribution of fungal matrix (*green*) and indigo pigment (*blue*). **A** *S. commune* hypha from an interaction between *S. commune* 12–43×4–39 and *H. fasciculare*, **B** hypha of *S. commune* F15, and **C** hypha of F15×F28, a ΔGap1/Δ Gap1 mutant dikaryon strain of *S. commune*. **D** End-member spectra of the three samples representing regions in *blue* (indigo) and *green* (fungal matrix) where (**a**) corresponds to the *blue-colored* areas, (**b**) corresponds to the *green regions*

The band at 1573 cm^{-1} is used as a marker for the identification of indigo [40]. All Raman bands of indigo are resonance enhanced, because of a coupling of the vibrational modes with an electronic transition. As a consequence, the band intensities of indigo are largely increased compared with the protein bands. Indigo was detected in the interaction zones of wild-type dikaryon 12–43×4–39 and wild type monokaryons 12–43 and 4–39 co-cultured with *H. fasciculare*, and in the mono culture of pigmented mutant F15. Indigo localization could also be observed in mono-cultured Δ*gap1*/Δ*gap1* dikaryon hyphae of *S. commune* (Fig. 5C). Isatin and indirubin could not be detected in these scans.

Discussion

The study of fungal interactions (albeit on artificial media), are important to gain an insight into the functionality of microorganisms on similar substrates (rotting wood) and their race for space and nutrient resources, which have greater implication in the forest ecosystem. In order to maintain fungal diversity in ecosystems, it is important to understand the underlying mechanisms determining the ecology of the fungal community [41]. White rot fungi produce a variety of compounds during interactions with other microorganisms. In this study, we have identified the colored metabolites produced by *S. commune* in interaction with *H. fasciculare* as indigo, indirubin, and isatin. Self-paired cultures did not show pigmentation, which is indicative of self-recognition. Although these compounds have been identified previously as being

produced by *S. commune* mutant strains, they have neither been found in wildtype *S. commune* cultures nor been reported in co-cultures of *S. commune* with other fungi. Indigo produced by pigmented *S. commune* mutants was first identified by Miles et al. [24]. However, several conditions are required for indigo production, related to carbon sources, temperature, and pH [42]. The fact that indigo was detected only in the co-cultures led us to assume that it is either a stress response or an indication of a defense response against antagonistic microorganisms. The possibility could also arise that *H. fasciculare* synthesizes an inhibitor towards *S. commune*, which detoxifies it, one product being indigo. The presence of lignin-modifying enzymes in *S. commune* seemed to increase the decolorization of individual commercial triarylmethane, anthraquinonic, and indigoid textile dyes by 25 % using enzyme preparations [43]. This indicated the ability of *S. commune* to detoxify selected harmful substances. Indirubin and isatin are known to be pharmacologically important [44] because they are potent inhibitors of cyclin dependent kinases, have anti-viral [45], anti-bacterial, and anti-fungal [46] activity among others.

Pigments, which appeared to be colored black and green also tested positive for indigo, meaning that the colors visualized were just a combination of concentration of the indigo secreted and its appearance in the media. The indigo and indirubin, produced in the cytoplasm of the hyphal cells are by-products of tryptophan catabolism and were transported along the cells. Staining of the pigmented hyphae with membrane stain FM4-64 did not show localization of indigo within vacuoles. Tryptophan is transformed to hydroxyanthranilic acids that become the precursor of phenoxazines and other

nitrogen-containing pigments [47] such as the indigoids. Various studies have reported the production of a variety of other indigoid derivatives by *S. commune*. Isatin and indirubin were found by Miles [24] and Epstein [48], respectively, in pigmented mutant strains of *S. commune*. Schizocommunin was isolated along with indigo, indirubin, isatin, and tryptanthrin, from the liquid culture medium in which a culture of *S. commune*, isolated from the bronchus of a human patient with allergic bronchopulmonary mycosis, had been grown [49].

There is a significant disparity in spatial resolution between LESA and Raman microscopy. The spatial resolution of Raman microscopy is in the order of less than 1 μm, and dependent on the wavelength of the laser, while that of LESA is about 1 mm and depends on solvent composition, volume dispensed on the surface and surface tension [50]. In order to keenly observe the interactions and compounds produced, we focused our UHPLC–ESI–MS/MS study on the *S. commune* 12–43×4–39–*H. fasciculare* pairing in liquid CYM media. The cell-free culture broth of mono-cultured *S. commune* and *H. fasciculare* had no effect on the other's growth and did not induce pigmentation. From this, we deduce that in this case mycelial contact is necessary for pigmentation. This extraction was done with methanol–water and the yield of the compounds obtained was low. Since the interactions could not be monitored well in the liquid cultures, we altered the culture method to solid agar co-cultures of the pairing and modified the extraction solvents to methanol–water–ethyl acetate. Thus, the interaction zone, as well as the zones at the periphery of either partner could be sampled easily and their metabolite profiles compared. The modified protocol resulted in higher yields of the compounds identified. In this study, we detected the production of indigo and indirubin in the amounts of 208 ± 66.76 pmol and 0.87 ± 0.23 pmol/cm^3 agar, respectively. Swack and Miles [42] obtained average indigo yields of 19.06–38.13 nmol/ml by pigmented mutants of *S. commune* in minimal media. Ujor et al. [30] conducted similar studies using gas chromatography–time of flight–mass spectrometry (GC–TOF–MS) for detection of the metabolites, however, the presence of indigoids were not reported. GC/MS requires the analytes to be in an organic injection solvent and derivatization is often necessary to improve peak shape, ionization, and/or volatility, LC–MS however does not. As a result, the primary advantage HPLC–MS has over GC/MS is that it is capable of analyzing a much wider range of components including compounds that are thermally labile, exhibit high polarity or have a high molecular mass [51]. The presence of isatin could be confirmed by MS/MS fragmentation. In the case of isatin fragmentation, the instrumentation was deemed important. Experiments to confirm isatin content showed that both sensitivity and fragmentation capacity of the trap (Orbitrap XL) was insufficient compared to HCID (Q Exactive Plus). The standard higher-energy collisional

dissociation (HCD) cell provides exceptional flexibility in fragmentation for advanced small-molecule research. Combining fast, sensitive linear ion trap MS^n with high-resolution, accurate-mass (HR/AM) Orbitrap™ technology optimizes precursor selection and transmission, improving quantitation of low-abundance ions in the most complex matrices.

Optimization of extraction is further considered necessary to increase the amounts of metabolites. Indigo, due to its high molecular symmetry and conjugated bond system, provides strong resonance-enhanced Raman signals [40]. The Raman spectra of indigo and indirubin reference compounds were distinct despite them being structural isomers (ESM Fig. S2). Raman microspectroscopy, exemplifies chemical imaging in a sense that it is a non-invasive label-free imaging technique. Indigo localization could even be imaged in $\Delta gap1/\Delta gap1$ mutant dikaryon hyphae of *S. commune*, which microscopically did not show any sign of the production of the pigment in its hyphae. The gene gap1 encodes a GTPase-activating protein for Ras. $\Delta gap1$ mutants are those in which the gene has been disrupted thus leading to production of phenotypes that are unable to maintain growth orientation and display altered clamp connections [52].

The indigo and indirubin molecules are uncharged and largely insoluble in most solvents. Raman spectroscopy has been shown to be a sensitive method to identify indigo even in the presence of pigment impurities [40]. Thus, we have shown that Raman microspectroscopy is an efficient tool to identify the presence of compounds, which have a relatively low solubility in water and organic solvents, without extensive sample preparation and measurement time. Alternatively, LESA–HRMS was performed to analyze fungal interactions without sample preparation. LESA was previously used to directly screen antibiotics from bacterial plates [53]. In our study, even though the mycelia covered the agar surface, the sample could be directly measured since the ethyl acetate solvent dissolved the mycelium. Therefore, there was no need to scrape the mycelium from the agar before extraction. The shortcoming that isobaric compounds as indigo and indirubin could not be differentiated by LESA–HRMS was hurdled by implementing UHPLC–HRMS. Using this technique, it has been demonstrated that there is about 200 fold more indigo present in the agar compared to indirubin. However, recently, an alternative generic approach to LC–MS has been described which integrates LESA for analytes tissue extraction followed by differential ion mobility spectrometry (DMS) mass spectrometry for analytes gas phase separation [54]. In combination, LESA–MS as a tool to rapidly extract, detect, and visualize natural products like indigoids directly from the sample without any preparation protocols, UHPLC–HRMS for verification and quantification of those metabolites, and Raman microspectroscopy to identify and image target compounds are powerful tools to study fungal interactions in situ.

This combination of methods is particularly useful in situations where application of matrix is impossible as the growing colonies have three-dimensional structure and are very fine. After matrix application, all structures will be disturbed and imaging will not be possible. On the other side, Raman imaging can be used for compounds showing vibrations distinguishable from the substrate background and the microorganism primary metabolites not involved in the studied interaction.

References

1. Moree WJ, Phelan VV, Wu C-H, Bandeira N, Cornett DS, Duggan BM, Dorrestein PC (2012) Interkingdom metabolic transformations captured by microbial imaging mass spectrometry. Proc Natl Acad Sci U S A 109(34):13811–13816

2. Watrous J, Roach P, Heath B, Alexandrov T, Laskin J, Dorrestein PC (2013) Metabolic profiling directly from the petri dish using nanospray desorption electrospray ionization imaging mass spectrometry. Anal Chem 85(21):10385–10391

3. Walter A, Erdmann S, Bocklitz T, Jung EM, Vogler N, Akimov D, Dietzek B, Rosch P, Kothe E, Popp J (2010) Analysis of the cytochrome distribution via linear and nonlinear Raman spectroscopy. Analyst 135(5):908–917

4. Popp J, Tuchin VV, Chiou A, Heinemann SH (2011) Volume 1: basics and techniques. Handbook of biophotonics. Chiou A HS, Popp J, Tučin VV (eds). Wiley-VCH

5. Kertesz V, Van Berkel GJ (2010) Fully automated liquid extraction-based surface sampling and ionization using a chip-based robotic nanoelectrospray platform. J Mass Spectrom 45(3):252–260

6. Harz M, Rosch P, Popp J (2009) Vibrational spectroscopy—a powerful tool for the rapid identification of microbial cells at the single-cell level. Cytometry A 75(2):104–113

7. Krafft C, Dietzek B, Popp J (2009) Raman and CARS microspectroscopy of cells and tissues. Analyst 134(6):1046–1057

8. Delhaye M, Dhamelincourt P (1975) Raman microprobe and microscope with laser excitation. J Raman Spectrosc 3(1):33–43

9. Tague T (2009) Infrared and Raman microscopy: pushing the limits of spatial resolution. Microsc Microanal 15(Supplement S2):562–563

10. Eikel D, Vavrek M, Smith S, Bason C, Yeh S, Korfmacher WA, Henion JD (2011) Liquid extraction surface analysis mass spectrometry (LESA-MS) as a novel profiling tool for drug distribution and metabolism analysis: the terfenadine example. Rapid Commun Mass Spectrom 25(23):3587–3596

11. Johnson D, Krsek M, Wellington EMH, Stott AW, Cole L, Bardgett RD, Read DJ, Leake JR (2005) Soil invertebrates disrupt carbon flow through fungal networks. Science 309(5737):1047

12. Lundell TK, Mäkelä MR, Hildén K (2010) Lignin-modifying enzymes in filamentous basidiomycetes—ecological, functional and phylogenetic review. J Basic Microbiol 50(1):5–20

13. Kirk TK, Farrell RL (1987) Enzymatic "combustion": the microbial degradation of lignin. Annu Rev Microbiol 41:465–505

14. Eriksson KEL, Blanchette RA, Ander P. (2012) Microbial and enzymatic degradation of wood and wood components. Springer London, Limited

15. Hatakka A (1994) Lignin-modifying enzymes from selected white-rot fungi: production and role from in lignin degradation. FEMS Microbiol Rev 13(2–3):125–135

16. Rayner ADM, Griffith GS, Howard GW (1994) Induction of metabolic and morphogenetic changed during mycelial interactions among species of higher fungi. Biochem Soc Trans 22:389–394

17. Rayner ADM, Webber JF (1984) Interspecific mycelial interactions—an overview. In: Jennings DH, Rayner ADM (eds) The ecology and physiology of the fungal mycelium. Cambridge University Press, Cambridge, pp 383–417

18. White NA, Boddy L (1992) Extracellular enzyme localization during interspecific fungal interactions. FEMS Microbiol Lett 98(1–3):75–79

19. Boddy L (2000) Interspecific combative interactions between wood-decaying basidiomycetes. FEMS Microbiol Ecol 31(3):185–194

20. Rayner ADM (1991) The challenge of the individualistic mycelium. Mycologia 83(1):48–71

21. Raudaskoski M, Kothe E (2010) Basidiomycete mating type genes and pheromone signaling. Eukaryot Cell 9(6):847–859

22. Ohm RA, de Jong JF, Lugones LG, Aerts A, Kothe E, Stajich JE, de Vries RP, Record E, Levasseur A, Baker SE, Bartholomew KA, Coutinho PM, Erdmann S, Fowler TJ, Gathman AC, Lombard V, Henrissat B, Knabe N, Kues U, Lilly WW, Lindquist E, Lucas S, Magnuson JK, Piumi F, Raudaskoski M, Salamov A, Schmutz J, Schwarze FW, vanKuyk PA, Horton JS, Grigoriev IV, Wosten HA (2010) Genome sequence of the model mushroom *Schizophyllum commune*. Nat Biotechnol 28(9):957–963

23. Papazian HP (1950) The physiology of the incompatibility factors in *Schizophyllum commune*. Bot Gaz 112:143–163

24. Miles PG, Lund H, Raper JR (1956) The identification of indigo as a pigment produced by a mutant culture of *Schizophyllum commune*. Arch Biochem Biophys 62(1):1–5

25. Willstaedt H (1935) Über die Farbstoffe des echten Reizkers (*Lactarius deliciosus* L.) (I. Mitteil.). Ber Dtsch Chem Ges A B Ser 68(2):333–340

26. Willstaedt H (1936) Über die Farbstoffe des echten Reizkers (*Lactarius deliciosus* L.) (II. Mitteil.). Ber Dtsch Chem Ges A B Ser 69(5):997–1001

27. Kögl F, Erxleben H, Jänecke L (1930) Untersuchungen über Pilzfarbstoffe. IX. Die Konstitution der Thelephorsäure. Justus Liebigs Ann Chem 482(1):105–119

28. Kögl F, Deijs WB (1935) Untersuchungen über Pilzfarbstoffe. XI. Über Boletol, den Farbstoff der blau anlaufenden Boleten. Justus Liebigs Ann Chem 515(1):10–23

29. Cartwright KSG, Findlay WPK (1946) Decay of timber and its prevention. Her Majesty's Stationary Office, London

30. Ujor VC, Monti M, Peiris DG, Clements MO, Hedger JN (2012) The mycelial response of the white-rot fungus, *Schizophyllum commune* to the biocontrol agent, *Trichoderma viride*. Fungal Biol 116(2):332–341

31. Schwalb MN, Miles PG (1967) Morphogenesis of *Schizophyllum commune*. II. Effect of microaerobic growth. Mycologia 59:610–622

32. Miljkovic M, Chernenko T, Romeo MJ, Bird B, Matthaus C, Diem M (2010) Label-free imaging of human cells: algorithms for image reconstruction of Raman hyperspectral datasets. Analyst 135(8):2002–2013

33. Hedegaard M, Matthäus C, Hassing S, Krafft C, Diem M, Popp J (2011) Spectral unmixing and clustering algorithms for assessment of single cells by Raman microscopic imaging. Theor Chem Accounts 130:1249–1260

34. Xia J, Mandal R, Sinelnikov IV, Broadhurst D, Wishart DS (2012) MetaboAnalyst 2.0—a comprehensive server for metabolomic data analysis. Nucleic Acids Res 40:W127–133, Web Server issue

35. Wang CS, Miles PG (1966) Studies of the cell walls of *Schizophyllum commune*. Am J Bot 53(8):792–800

36. Tuma R (2005) Raman spectroscopy of proteins: from peptides to large assemblies. J Raman Spectrosc 36(4):307–319

37. Zhang K, Geissler A, Fischer S, Brendler E, Bäucker E (2012) Solid-state spectroscopic characterization of α-chitins deacetylated in homogeneous solutions. J Phys Chem B 116(15):4584–4592

38. Lee CM, Cho E-M, Yang SI, Ganbold E-O, Jun J, Cho K-H (2013) Raman spectroscopy and density functional theory calculations of β-glucans and chitins in fungal cell walls. Bull Korean Chem Soc 34(3): 943–945

39. Bauer H, Kowski K, Kuhn H, Lüttke W, Rademacher P (1998) Photoelectron spectra and electronic structures of some indigo dyes. J Mol Struct 445(1–3):277–286

40. Baran A, Fiedler A, Schulz H, Baranska M (2010) In situ Raman and IR spectroscopic analysis of indigo dye. Anal Methods 2(9):1372

41. Falconer RE, Bown JL, White NA, Crawford JW (2008) Modelling interactions in fungi. J R Soc Interface 5(23):603–615

42. Swack NS, Miles PG (1960) Conditions affecting growth and indigotin production by strain 130 of Schizophyllum commune. Mycologia 52(4):574–583

43. Abadulla E, Robra K-H, Gübitz GM, Silva LM, Cavaco-Paulo A (2000) Enzymatic decolorization of textile dyeing effluents. Textile Res J 70(5):409–414

44. Medvedev A, Buneeva O, Glover V (2007) Biological targets for isatin and its analogues: implications for therapy. Biologics 1(2):151–162

45. Sriram D, Bal TR, Yogeeswari P (2004) Design, synthesis and biological evaluation of novel non-nucleoside HIV-1 reverse transcriptase inhibitors with broad-spectrum chemotherapeutic properties. Bioorg Med Chem 12(22):5865–5873

46. Chohan ZH, Pervez H, Rauf A, Khan KM, Supuran CT (2004) Isatin-derived antibacterial and antifungal compounds and their transition metal complexes. J Enzyme Inhib Med Chem 19(5):417–423

47. Velišek J, Cejpek K (2011) Pigments of higher fungi—a review. Czech J Food Sci 29:87–102

48. Epstein E, Miles P (1966) Identification of indirubin as a pigment produced by mutant cultures of the fungus Schizophyllum commune. J Plant Res 79:566–571

49. Hosoe T, Nozawa K, Kawahara N, Fukushima K, Nishimura K, Miyaji M, Kawai K (1999) Isolation of a new potent cytotoxic pigment along with indigotin from the pathogenic basidiomycetous fungus Schizophyllum commune. Mycopathologia 146(1):9–12

50. Henion J, Eikel D, Linehan SL, Heller D, Murphy K, Rudewicz PJ & Prosser SJ (2011) Liquid extraction surface analysis mass spectrometry (LESA MS) - drug distribution and metabolism of diclofenac in the mouse. in 59th Conference of the American Society for Mass Spectrometry. Denver

51. Agilent Technologies I. Considerations for selecting GC/MS or LC/MS for metabolomics. 2007; Available from: http://www.chem.agilent.com/Library/selectionguide/Public/5989-6328EN.pdf

52. Schubert D, Raudaskoski M, Knabe N, Kothe E (2006) Ras GTPase-activating protein gap1 of the homobasidiomycete Schizophyllum commune regulates hyphal growth orientation and sexual development. Eukaryot Cell 5(4):683–695

53. Kai M, Gonzalez I, Genilloud O, Singh SB, Svatos A (2012) Direct mass spectrometric screening of antibiotics from bacterial surfaces using liquid extraction surface analysis. Rapid Commun Mass Spectrom 26(20):2477–2482

54. Porta T, Varesio E, Hopfgartner G (2013) Gas-phase separation of drugs and metabolites using modifier-assisted differential ion mobility spectrometry hyphenated to liquid extraction surface analysis and mass spectrometry. Anal Chem 85(24):11771–11779